JOC Article

Donor−Acceptor-Substituted Tetrakis(phenylethynyl)benzenes as Emissive Molecules during Pulse Radiolysis in Benzene

Shingo Samori, Sachiko Tojo, Mamoru Fujitsuka, Eric L. Spitler,† Michael M. Haley,† and Tetsuro Majima*

The Institute of Scientific and Industrial Research (SANKEN), Osaka University, Mihogaoka 8-1, Ibaraki, Osaka 567-0047, Japan, and Department of Chemistry and the Materials Science Institute, University of Oregon, Eugene, Oregon 97403-1253

majima@sanken.osaka-u.ac.jp

Received November 12, 2006

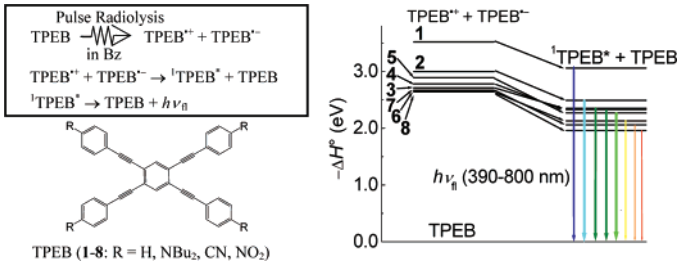

Emission from charge recombination between radical cations and anions of various tetrakis(phenylethynyl)-benzenes (TPEBs) was measured during pulse radiolysis in benzene (Bz). The formation of TPEB in the singlet excited state (^{1}TPEB*) can be attributed to the charge recombination between TPEB$^{\bullet+}$ and TPEB$^{\bullet-}$, which are initially generated from the radiolytic reaction in Bz. This mechanism is reasonably explained by the relationship between the annihilation enthalpy change ($-\Delta H°$) for the charge recombination of TPEB$^{\bullet+}$ and TPEB$^{\bullet-}$ and excitation energy of ^{1}TPEB*. It was found that the charge recombination between TPEB$^{\bullet+}$ and TPEB$^{\bullet-}$ occurred to give ^{1}TPEB* as the emissive species, but not the excimers because of the large repulsion between substituents caused by the rotation around C−C single bonds of TPEBs. Since donor−acceptor-substituted TPEBs possess three types of charge-transfer pathways (linear-conjugated, cross-conjugated, and "bent" conjugated pathways between the donor and acceptor substituents through the ethynyl linkage), the emission spectra of ^{1}TPEBs* with intramolecular charge transfer (ICT) character depend on the substitution pattern and the various kinds of donor and acceptor groups during pulse radiolysis in Bz.

Introduction

Electron detachment from and attachment to a solute molecule (M) generates radical cations (M$^{\bullet+}$) and anions (M$^{\bullet-}$), respectively. M$^{\bullet+}$ and M$^{\bullet-}$ are known as important ionic intermediates in photochemistry, electrochemistry, and radiation chemistry.[1] It is well-known that M in the excited states (M* = ^{1}M* (singlet excited state) and ^{3}M* (triplet excited state)) can be formed by charge recombination between M$^{\bullet+}$ and M$^{\bullet-}$ (M$^{\bullet+}$ + M$^{\bullet-}$ → M* + M), after which ^{1}M* deactivates to M in the ground state by emitting light (^{1}M* → M + $h\nu_{fl}$).[2] This process is significant for optoelectronic materials such as OLEDs because electrochemical energies can be converted to photochemical energies.

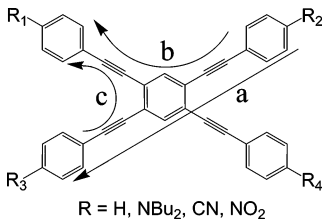

FIGURE 1. Three types of charge-transfer conjugated pathway in TPEBs are shown by arrows.

Recently, organic compounds possessing a high degree of π-conjugation with donor and/or acceptor groups have been

* To whom correspondence should be addressed. Tel: +6-6879-8495. Fax: +6-6879-8499.
† University of Oregon.

(1) (a) Fox, M. A.; Chanon, M. *Photoinduced Electron Transfer*; Elsevier: Amsterdam, 1988. (b) Kavarnos, G. J.; Turro, N. J. *Chem. Rev.* **1986**, *86*, 401.

10.1021/jo062326h CCC: $37.00
Published on Web 03/17/2007

SCHEME 1

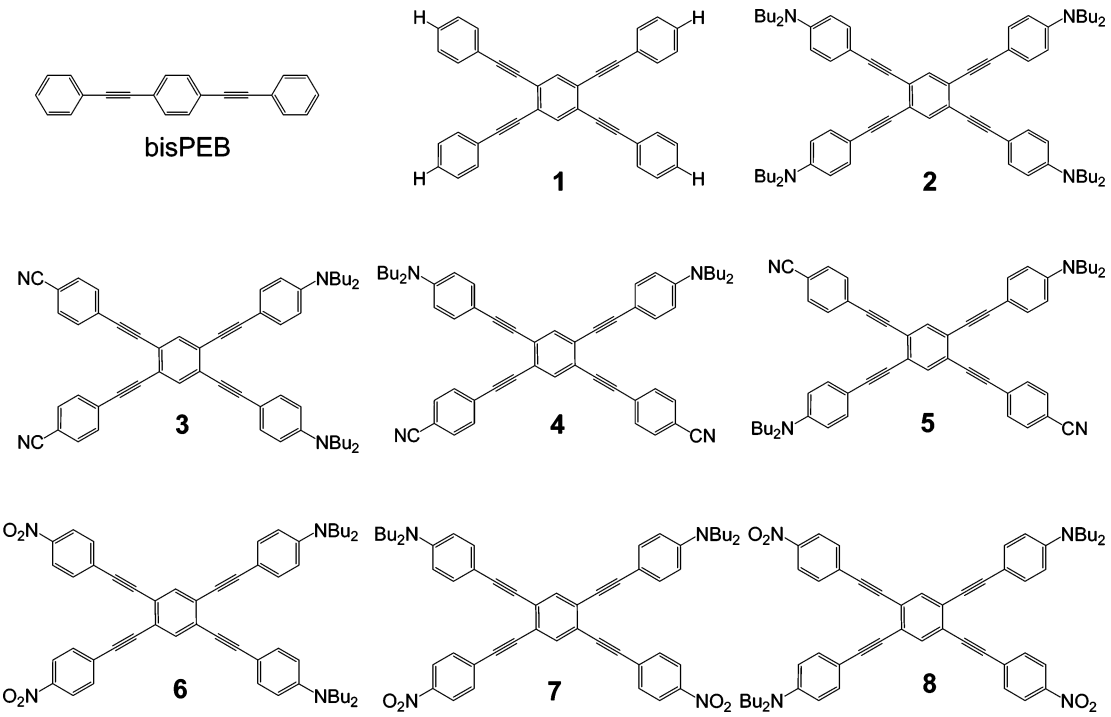

recognized as ideal materials for optoelectronic applications.[3−5] Changes in the substituents and substitution pattern, electronic structure, and conjugation can provide highly variable photophysical properties for such materials. Therefore, it is expected that detailed study on the structure−property relationships for these materials will provide valuable information for molecular design with high performance.

As a class of π-conjugated molecules with remarkable optoelectronic properties, functionalized cruciform-conjugated phenylacetylene structures have received considerable attention because of their multiple conjugated pathways.[5−7] The 1,2,4,5-tetrakis(substituted phenylethynyl)benzene (TPEB) framework is an ideal system for studying the differences between the linear-conjugated (Figure 1, path a), cross-conjugated (path b), and "bent" conjugated (path c) pathways to gain a better understanding of the geometrical aspects of the charge-transfer pathways. By varying the substitution pattern of the donor and acceptor groups, each charge-transfer pathway can be modified. It has been previously shown that linear conjugation between donor and acceptor groups is ideal for lowering the HOMO−LUMO gap for charge-transfer, thereby enhancing the optical and nonlinear optical properties of the material.[5−8]

In this paper, we report the emission from the charge recombination between $TPEB^{\bullet+}$ and $TPEB^{\bullet-}$ of various tetrakis(phenylethynyl)benzenes (TPEBs = **1**−**8**): 1,2,4,5-tetrakis(phenylethynyl)benzene **1** (neutral), 1,2,4,5-tetrakis(*N*,*N*-dibutylaminophenyl)benzene **2** (tetra-donor TPEB), and regioisomeric donor−acceptor substituted 1,2,4,5-tetrakis(phenylethynyl)benzenes with donating *N*,*N*-dibutylamino and accepting cyano or

(2) (a) Faulkner, L. R.; Bard, A. J. *Electroanalylical Chemistry*; Marcel Dekker: New York, 1977; Vol. 10, pp 1−95. (b) Bard, A. J.; Faulkner, L. R. *Electrochemical Methods Fundamentals and Applications*, 2nd ed.; John Wiley and Sons: New York, 2001; pp 736−745. (c) Richter, M. M. *Chem. Rev.* **2004**, *104*, 3003.

(3) (a) Goes, M.; Verhoeven, J. W.; Hofstraat, H.; Brunner, K. *ChemPhysChem* **2003**, *4*, 349. (b) Thomas, K. R. J.; Lin, J. T.; Tao, Y.-T.; Chuen, C.-H. *Chem. Mater.* **2002**, *14*, 3852. (c) Zhu, W.; Hu, M.; Yao, R.; Tian, H. *J. Photochem. Photobiol., A* **2003**, *154*, 169. (d) Thomas, K. R. J.; Lin, J. T.; Velusamy, M.; Tao, Y.-T.; Chuen, C.-H. *Adv. Funct. Mater.* **2004**, *14*, 83. (e) Chiang, C.-L.; Wu, M.-F.; Dai, D.-C.; Wen, Y.-S.; Wang, J.-K.; Chen, C.-T. *Adv. Funct. Mater.* **2005**, *15*, 231.

(4) (a) Elangovan, A.; Chen, T.-Y.; Chen, C.-Y.; Ho, T.-I. *Chem. Commun.* **2003**, 2146. (b) Elangovan, A.; Yang, S.-W.; Lin, J.-H.; Kao, K.-M.; Ho, T.-I. *Org. Biomol. Chem.* **2004**, *2*, 1597. (c) Elangovan, A.; Chiu, H.-H.;Yang, S.-W.; Ho, T.-I. *Org. Biomol. Chem.* **2004**, *2*, 3113. (d) Elangovan, A.; Kao, K.-M.; Yang, S.-W.; Chen, Y.-L.; Ho, T.-I.; Su, Y. O. *J. Org. Chem.* **2005**, *70*, 4460. (e) Yang, S.-W.; Elangovan, A.; Hwang, K.-C.; Ho, T.-I. *J. Phys. Chem. B* **2005**, *109*, 16628. (f) Lin, J.-H.; Elangovan, A.; Ho, T.-I. *J. Org. Chem.* **2005**, *70*, 7397.

(5) (a) Jayakannan, M.; Van Hal, P. A.; Janssen, R. A. J. *J. Polym. Sci., Part A: Polym. Chem.* **2001**, *40*, 251. (b) Tykwinski, R. R.; Schreiber, M.; Carlon, R. P.; Diederich, F.; Gramlich, V. *Helv. Chim. Acta* **1996**, *79*, 2249. (c) Tykwinski, R. R.; Schreiber, M.; Gramlich, V.; Seiler, P.; Diederich, F. *Adv. Mater.* **1996**, *8*, 226. (d) Wilson, J. N.; Hardcastle, K. I.; Josowicz, M.; Bunz, U. H. F. *Tetrahedron.* **2004**, *60*, 7157. (e) Wilson, J. N.; Smith, M. D.; Enkelmann, V.; Bunz, U. H. F. *Chem. Commun.* **2004**, 1700. (f) Wilson, J. N.; Josowicz, M.; Wang, Y.; Bunz, U. H. F. *Chem. Commun.* **2003**, 2962. (g) Miteva, T.; Palmer, L.; Kloppenburg, L.; Neher, D.; Bunz, U. H. F. *Macromolecules* **2000**, *33*, 652. (h) Zucchero, A. J.; Wilson, J. N.; Bunz, U. H. F. *J. Am. Chem. Soc.* **2006**, *128*, 11872. (i) Ojima, J.; Kakumi, H.; Kitatani, K.; Wada, K.; Ejiri, E.; Nakada, T. *Can. J. Chem.* **1984**, *63*, 2885. (j) Ojima, J.; Enkaku, M.; Uwai, C. *Bull. Chem. Soc. Jpn.* **1977**, *50*, 933.

(6) (a) Miller, J. J.; Marsden, J. A.; Haley, M. M.; *Synlett* **2004**, 165. (b) Marsden, J. A.; Miller, J. J.; Shirtcliff, L. D.; Haley, M. M.; *J. Am. Chem. Soc.* **2005**, *127*, 2464.

(7) (a) Marsden, J. A.; Palmer, G. J.; Haley, M. M. *Eur. J. Org. Chem.* **2003**, 2355. (b) Jones, C. S.; O'Connor, M. J.; Haley, M. M. In *Acetylene Chemistry: Chemistry, Biology, and Materials Science*; Diederich, F., Tykwinski, R. R., Stang, P. J., Eds.; Wiley-VCH: Weinheim, Germany, 2004; pp 303−385. (c) Marsden, J. A.; Haley, M. M. *J. Org. Chem.* **2005**, *70*, 10213. (d) Anand, S.; Varnavski, O.; Marsden, J. A.; Haley, M. M.; Schlegel, H. B.; Goodson, T., III. *J. Phys. Chem. A* **2006**, *110*, 1305. (e) Bhaskar, A.; Guda, R.; Haley, M. M.; Goodson, T., III. *J. Am. Chem. Soc.* **2006**, *128*, 13972. (f) Slepkov, A. D.; Hegmann, F. A.; Tykwinski, R. R.; Kamada, K.; Ohta, K.; Marsden, J. A.; Spitler, E. L.; Miller, J. J., Haley, M. M. *Opt. Lett.* **2006**, *31*, 3315. (g) Spitler, E. L.; Shirtcliff, L. D.; Haley, M. M. *J. Org. Chem.* **2006**, *72*, 86.

(8) (a) Hilger, A.; Gisselbrecht, J. P.; Tykwinski, R. R.; Boudon, C.; Schreiber, M.; Martin, R. E.; Luthi, H. P.; Gross, M.; Diederich, F. *J. Am. Chem. Soc.* **1997**, *119*, 2069. (b) Kondo, K.; Yasuda, S.; Tohoru, S.; Miya, M. *J. Chem. Soc., Chem. Commun.* **1995**, 55.

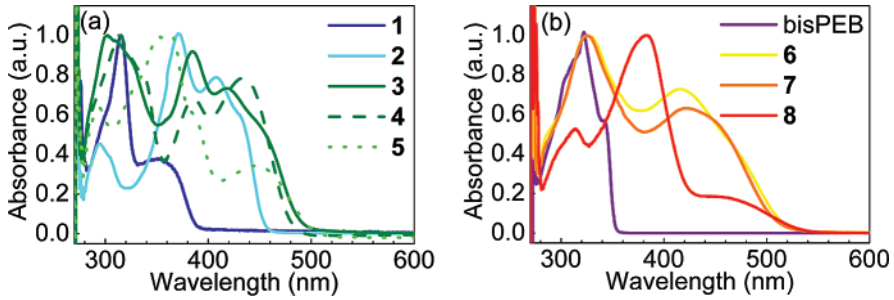

FIGURE 2. Absorption ((a) and (b)) spectra observed by the steady-state measurement of TPEBs (**1**−**8**) and bisPEB in Ar-saturated Bz. All solutions were prepared at a dilute concentration (10^{-5} M).

nitro groups **3**−**8** (donor−acceptor TPEB).[6] Chemical structures of TPEBs are shown in Scheme 1. Donor−acceptor type TPEBs (**3**−**8**) have two donor and two acceptor groups with like substituents fused either ortho (**3** and **6**), meta (**4** and **7**), or para (**5** and **8**) to each other. In addition, 1,4-bis(phenylethynyl)-benzene (bisPEB) was examined as the parent molecule.

In recent years, we have proposed the emission mechanisms of donor−acceptor type molecules with an ethynyl linkage (DEA) such as phenylquinolinylethynes,[9a] phenyl(9-acridinyl)-ethynes,[9b] phenyl(9-cyanoanthracenyl)ethynes,[9b,d] and arylethynylpyrenes[9c] during the pulse radiolysis in benzene (Bz). Most DEAs exhibit electrogenerated chemiluminescence (ECL), which originates from charge recombination between $DEA^{\bullet+}$ and $DEA^{\bullet-}$ in solution.[4] Using the pulse radiolysis technique, both $DEA^{\bullet+}$ and $DEA^{\bullet-}$ can be generated at the same time in Bz. We found that charge recombination between $DEA^{\bullet+}$ and $DEA^{\bullet-}$ occurred to give DEA in the lowest singlet excited state (S_1) ($^1DEA^*$) and/or singlet excimer ($^1DEA_2^*$) as the emissive species during the pulse radiolysis in Bz, for the first time. Since DEAs have electron donor and acceptor substituents at both ends of the ethynyl linkage, they possess charge-transfer character through the linear-conjugated pathway (a). For DEAs with strong electron-donor character and bulky substituents (for instance, 9-cyano-10-(*N*,*N*-di-*p*-anisylamino)phenylethynyl-anthracene),[9d] a considerably twisted structure is assumed to give $^1DEA^*$ with strong intramolecular charge transfer (ICT) character but not $^1DEA_2^*$ because of the bulky donor substituent. These molecules are useful as luminescent materials because a judicious choice of the donor/acceptor unit can allow the control of the HOMO−LUMO levels and thus the emission color can be obtained in the visible region.[4] In fact, different donor and acceptor substituents can change the emission color and intensity to some extent. However, fine-tuning of the emission color and intensity seems to be difficult for donor−acceptor-type DEAs because they possess only linear-conjugated pathway (a). Some DEAs showed the excimer emission with less luminescence intensity during the pulse radiolysis,[9b−d] although they are not suitable for luminescent materials.

Since three different types of charge-transfer conjugated pathways are known for individual donor−acceptor substituted TPEBs as described above, we can easily fine-tune the emission color and intensity by changing the substitution pattern and the various kinds of donor and acceptor substituents. These compounds are also useful for luminescent materials because most of them exhibit sufficient emission efficiency in the region of visible light. In addition, TPEBs can rotate freely about their C−C single bonds,[6] decreasing π-orbital overlap, and thus formation of the face-to-face excimer structure with less luminescence intensity cannot be expected during the pulse radiolysis in Bz. The time-resolved transient absorption and emission measurements during the pulse radiolysis of various TPEBs are useful to gain a better understanding of the emission mechanism, providing valuable information for molecular design with efficient luminescence character.

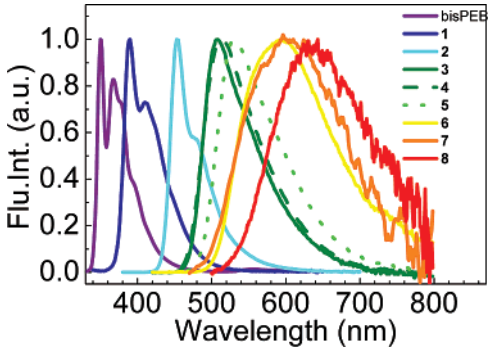

FIGURE 3. Fluorescence spectra observed by the steady-state measurement of TPEBs (**1**−**8**) and bisPEB in Ar-saturated Bz. All solutions were prepared at a dilute concentration (10^{-5} M).

Results and Discussion

Steady-State Spectral Properties of TPEBs. Normalized steady-state absorption and fluorescence spectra of TPEBs in Bz are shown in Figures 2 and 3, respectively. All TPEBs showed a characteristic pattern with broad absorption bands as shown in Figure 2a,b. Compared to neutral **1**, tetradonor **2** showed a large red shift (∼60 nm) of these bands. TPEBs **1** and **2** exhibit a characteristic $\pi-\pi^*$ transition from the HOMO to LUMO. On the other hand, the corresponding absorption bands of the donor−acceptor-substituted TPEBs (**3**−**8**) are remarkably broadened and show further bathochromic shifts, indicating the charge transfer from the donor to the acceptor for the HOMO−LUMO transition.[6] TPEBs **3**, **4**, **6**, and **7**, which possess linear-conjugated pathways, have a much more distinct low-energy band. Lacking the linear charge-transfer linkage, the low energy band of TPEBs **5** and **8** is weakened. This further indicates that linear-conjugated pathways are more efficient than the "bent" conjugated or cross-conjugated donor to acceptor pathways.[6]

(9) (a) Samori, S.; Hara, M.; Tojo, S.; Fujitsuka, M.; Yang, S.-W.; Elangovan, A.; Ho, T.-I.; Majima, T. *J. Phys. Chem. B* **2005**, *109*, 11735. (b) Samori, S.; Tojo, S.; Fujitsuka, M.; Yang, S.-W.; Elangovan, A.; Ho, T.-I.; Majima, T. *J. Org. Chem.* **2005**, *70*, 6661. (c) Samori, S.; Tojo, S.; Fujitsuka, M.; Yang, S.-W.; Ho, T.-I.; Yang, J.-S.; Majima, T. *J. Phys. Chem. B* **2006**, *110*, 13296. (d) Samori, S.; Tojo, S.; Fujitsuka, M.; Liang, H.-J.; Ho, T.-I.; Yang, J.-S.; Yang, S.-W.; Majima, T. *J. Org. Chem.* **2006**, *71*, 8732.

TABLE 1. Steady-State Spectral Properties of TPEBs (1−8) and bisPEB in Ar-Saturated Bz

compd	λ_{max}^{Abs} (nm)	λ_{max}^{Fl} (nm)	Stokes shift (nm)	E_{S1}[a] (eV)	ϕ_{fl}	τ_{fl} (ns)
1	315, 351	390	39	3.18	0.70 ± 0.03	2.3
2	371, 408	453	45	2.74	0.95 ± 0.01	1.9
3	302, 385, 418	508	90	2.44	0.73 ± 0.02	4.1
4	313, 386, 435	512	77	2.42	0.62 ± 0.02	4.5
5	352, 364, 446	530	84	2.34	0.53 ± 0.02	6.2
6	326, 417	594	177	2.09	0.36 ± 0.01	3.6
7	325, 421	610	189	2.03	$(5.1 \pm 0.2) \times 10^{-3}$	2.0
8	313, 383, 446	643	197	1.93	$(4.8 \pm 0.1) \times 10^{-4}$	0.067
bisPEB	320	350	30	3.54	0.90 ± 0.02	0.65

[a] Estimated from the peak wavelength of the fluorescence spectra (10^{-5} M).

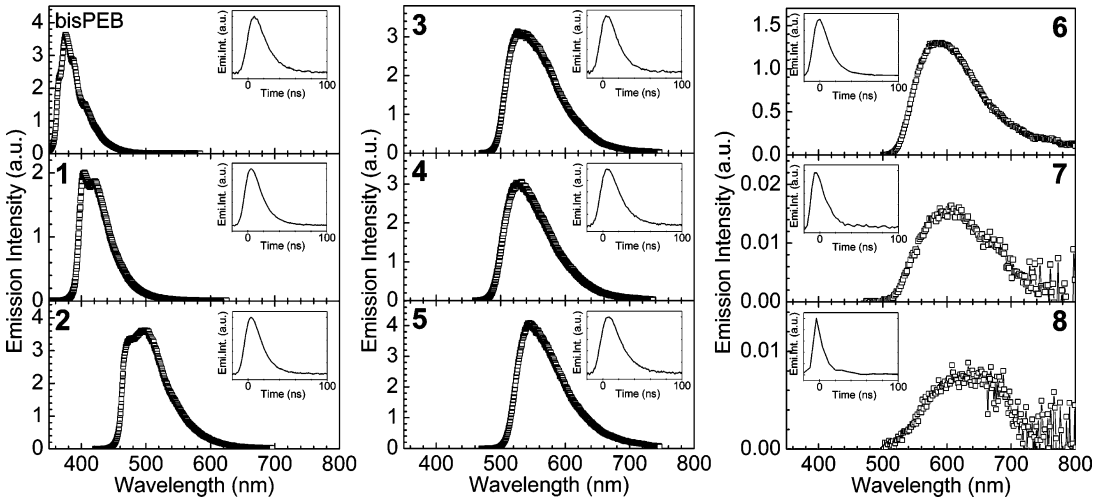

FIGURE 4. Emission spectra observed in the time range of 0−100 ns during the pulse radiolysis of TPEBs in Ar-saturated Bz (0.5 mM). Insets: time profiles of the emission observed at the emission peak.

Strong fluorescence was observed for the majority of TPEBs (Figure 3) and bisPEB. Compared to neutral **1** or tetradonor **2**, donor−acceptor TPEBs (**3**−**8**) showed a large red shift in the emission maxima in Bz. This again indicates ICT character for donor−acceptor substituted TPEBs in the S_1 state (Table 1). Discrete differences in emission energy, fluorescence quantum yield (ϕ_{fl}), and fluorescence lifetime (τ_{fl}) based on the molecular electronic structure and planarity of TPEBs and bisPEB were observed. The ϕ_{fl} value of **2** is highest (0.95 ± 0.01) and that of **8** is lowest ((4.8 ± 0.1) × 10^{-4}) in Ar-saturated Bz. In particular, ϕ_{fl} values of **7** ((5.1 ± 0.2) × 10^{-3}) and **8** are significantly lower than those of other TPEBs ((0.36 ± 0.01)−(0.95 ± 0.01)). Low ϕ_{fl} values of **7** and **8** can be attributed to small radiative rates of these compounds ((2.6−7.2) × 10^6 s^{-1}) compared with other TPEBs ((0.85−5.0) × 10^8 s^{-1}). As another factor for the low ϕ_{fl} values of **7** and **8**, internal conversion rate should be considered. From the peak positions of the fluorescence spectra of **7** and **8**, the excitation energies of ^{1}**7*** and ^{1}**8*** (E_{S1} = 2.03 and 1.93 eV, respectively) are estimated to be smaller than those of other ^{1}TPEBs* (2.09−3.18 eV). Thus, internal conversion rates of **7** and **8** will be faster than those of other TPEBs.[7g] Both decrease of radiative rate and increase of internal conversion rate are responsible for the low ϕ_{fl} values of **7** and **8**.

Obvious differences in fluorescence peaks were observed depending on the substitution pattern of the donor and/or acceptor groups. Compared to TPEBs with CN-acceptor substituents (**3**−**5**), the emission maxima of TPEBs with NO_2-acceptor substituents (**6**−**8**) were observed at longer wavelengths, since the electron withdrawing character of the NO_2-acceptor substituent is stronger than that of the CN acceptor. Since the electron-withdrawing and -donating character of the acceptor and donor substituents, respectively, govern the emission wavelength, a broad range of emission color and intensity of donor−acceptor-substituted TPEBs can be easily fine-tuned through control of the structural elements of the molecules.

Emission Generated from Charge Recombination between TPEB$^{\bullet+}$ and TPEB$^{\bullet-}$. Emission spectra were observed after an electron pulse during the pulse radiolysis of TPEBs in Ar-saturated Bz (0.5 mM). The emission of TPEBs indicates generation of ^{1}TPEBs* by charge recombination of TPEB$^{\bullet+}$ and TPEB$^{\bullet-}$ generated during pulse radiolysis in Bz as discussed in the later section. TPEBs showed emission peaks at 405−640 nm and bisPEB did at 376 nm during the pulse radiolysis (Figure 4). The emission maxima of donor−acceptor substituted TPEBs (**3**−**8**) were observed at longer wavelengths than neutral **1** or tetra-donor **2**, indicating ICT character in the S_1 state. In addition, the shape of the emission spectra of TPEBs and bisPEB were different from those observed in the steady-state measurements, and emission maxima observed at the shorter wavelength region disappeared because of strong self-absorption as a result of the high concentrations.[9] The radiolysis induced emission intensities of TPEBs and bisPEB (0.5 mM) in Table 2 were determined by correcting the self-absorption.

The insets in Figure 4 show the monotonous decay profiles of the emission with no delayed fluorescence resulted from triplet−triplet annihilation[9] during the pulse radiolysis of all TPEBs and bisPEB in Ar-saturated Bz. Therefore, the fluorescence lifetimes of all TPEBs and bisPEB were shorter than 8 ns. Figure 5 shows the emission time profiles observed at 527

TABLE 2. Emission Maxima (λ_{max}^{Em}) and Relative and Corrected Emission Intensities during the Pulse Radiolysis of TPEBs (1−8) and bisPEB in Ar-Saturated Bz (0.5 mM)

compd	λ_{max}^{Em} (nm)	relative intensity[a] (%)	corrected intensity[b] (%)
1	405	61.4	96.6
2	498	115	181
3	527	93.8	136
4	532	88.1	104
5	546	109	140
6	582	44.2	52.1
7	606	0.560	0.630
8	640	0.268	0.335
bisPEB	376	100	139

[a] Relative to the emission intensity of bisPEB in Ar-saturated Bz. Emission intensity was determined from the total amount of emission. [b] Since the emission intensities of all TPEBs and bisPEB are lower than those true values due to the strong self-absorption, emission intensity values are corrected on the basis of the fluorescence spectra obtained by the steady-state measurement.

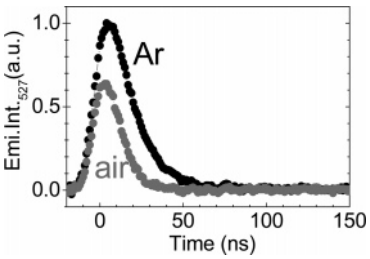

FIGURE 5. Time profiles of emission at 527 nm observed during the pulse radiolysis of **3** in Ar- and air-saturated Bz (black and gray colors, respectively).

nm during the pulse radiolysis of **3** in Ar- and air-saturated Bz. When air including oxygen was added to the solution, the initial emission intensity of the time profiles was reduced although there was no significant difference in the fluorescence lifetimes. The oxygen concentration in air-saturated organic solvent is only ∼1 mM, which is not sufficient to quench the fluorescence of TPEBs completely within 8-ns pulse duration by the bimolecular dynamic process. Therefore, assuming that initially formed electrons, which react with TPEB to form $TPEB^{\bullet-}$, were scavenged by O_2 within the spur, the reduction of fluorescence intensity can be explained. When N_2O gas was added in the solution as the electron scavenger, the reduction of the emission intensity was observed for TPEBs, which is also a strong indicator of the electron scavenging within the spur. As the similar examples, the hydrated electron (e_{aq}^-) is known to react with O_2 within the spur.[14] Since the oxygen concentration within

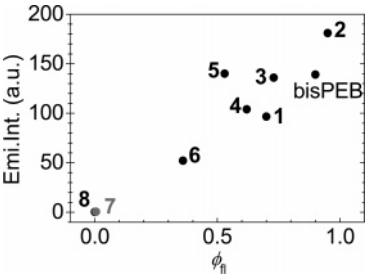

FIGURE 6. Plot of corrected emission intensity vs ϕ_{fl} for TPEBs **1**−**8** and bisPEB in Bz. Data points for **7** and **8** are overlapped.

TABLE 3. Electrochemical Properties of TPEBs and bisPEB in CH_3CN and Annihilation Enthalpy Changes ($-\Delta H°$), E'_{S1}, and ($-\Delta H° - E'_{S1}$) of TPEBs and bisPEB in Bz

	in CH_3CN		in Bz		
compd	E_{ox} (V)	E_{red} (V)	$-\Delta H°$ (eV)	E'_{S1}[b] (eV)	$-\Delta H° - E'_{S1}$ (eV)
1	1.37	−1.96	3.52	3.06	0.46
2	0.76	−2.05	3.00	2.49	0.51
3	0.49	−2.03	2.71	2.35	0.36
4	0.54	−2.05	2.78	2.33	0.45
5	0.55	−2.15	2.89	2.27	0.62
6	0.53	−1.93	2.65	2.13	0.52
7	0.53	−1.95	2.67	2.05	0.62
8	0.48	−1.97	2.64	1.94	0.70
bisPEB	1.38[a]	−2.35[a]	3.92	3.30	0.62

[a] Reference 11. [b] E'_{S1} values were determined from the peak wavelength of the radiolysis-induced emission spectra.

spur assumed to be lower than TPEB radical ion concentrations (∼0.1 M), complete disappearance of the fluorescence was not observed. The same emission behavior was observed for all TPEBs and bisPEB. This result clearly suggests that radical cation and anion are responsible for the emission during the pulse radiolysis.

Figure 6 shows the plots of corrected emission intensity vs ϕ_{fl} values for TPEBs and bisPEB in Bz. The radiolysis induced emission intensity of **2** was highest (181) and that of **8** was lowest (0.335) at 0.5 mM in Ar-saturated Bz. This tendency is the same as the ϕ_{fl} values, i.e., ϕ_{fl} value of **2** was the highest while that of **8** was the lowest. Considerable self-absorption was observed for **2**, **3**, and bisPEB, since the absorption and fluorescence spectra overlap well for these compounds. It was also found that the emission intensity of **5** (140) was higher than those of **3** (136) and **4** (104), although the ϕ_{fl} value of **5** (0.53) was lower than those of **3** (0.73) and **4** (0.62). Therefore, except for **5**, it can be suggested that the radiolysis-induced emission intensities of TPEBs depend on their ϕ_{fl} values.[9]

For some donor−acceptor-type molecules with an ethynyl linkage (DEA) prepared in high concentration, excimer emission has been observed during pulse radiolysis in Bz.[9b−d] At high concentration (5−10 mM), however, no excimer emission was observed during the pulse radiolysis of all TPEBs. Since TPEBs can rotate freely about their C−C single bonds, the decrease of π-orbital overlap is assumed. Therefore, the face-to-face interaction between $TPEB^{\bullet+}$ and $TPEB^{\bullet-}$ in the charge recombination cannot be allowed, and thus, formation of an excimer structure with less luminescence is assumed not to be observed during the pulse radiolysis in Bz.

Next, to elucidate the emission mechanism of TPEBs, the electrochemical properties (oxidation and reduction potentials)

(10) Gross, E. M.; Anderson, J. D.; Slaterbeck, A. F.; Thayumanavan, S.; Barlow, S.; Zhang, Y.; Marder, S. R.; Hall, H. K.; Nabor, M. F.; Wang, J.-F.; Mash, E. A.; Armstrong, N. R.; Wightman, R. M., *J. Am. Chem. Soc.* **2000**, *122*, 4972.

(11) Kilsa, K.; Kajanus, J.; Macpherson, A. N.; Martensson, J.; Albinsson, B. *J. Am. Chem. Soc.* **2001**, *123*, 3069.

(12) (a) Shida, T.; Hamill, W. H. *J. Chem. Phys.* **1966**, *44*, 2369, 2375, 3472. (b) Shida, T.; Kato, T. *Chem. Phys. Lett.* **1979**, *68*, 106. (c) Grimison, A.; Simpson, G. A. *J. Phys. Chem.* **1968**, *72*, 1776. (d) Ishida, A.; Fukui, M.; Ogawa, H.; Tojo, S.; Majima, T.; Takamuku, S. *J. Phys. Chem.* **1995**, *99*, 10808. (e) Majima, T.; Tojo, S.; Ishida, A.; Takamuku, S. *J. Org. Chem.* **1996**, *61*, 7793. (f) Majima, T.; Tojo, S.; Ishida, A.; Takamuku, S. *J. Phys. Chem.* **1996**, *100*, 13615.

(13) (a) Honda, E.; Tokuda, M.; Yoshida, H.; Ogasawara, M. *Bull. Chem. Soc. Jpn.* **1987**, *60*, 851. (b) Huddleston, R. K.; Miller, J. R. *J. Phys. Chem.* **1982**, *86*, 2410. (c) Majima, T.; Fukui, M.; Ishida, A.; Takamuku, S. *J. Phys. Chem.* **1996**, *100*, 8913. (d) Majima, T.; Tojo, S.; Takamuku, S. *J. Phys. Chem. A* **1997**, *101*, 1048.

(14) Tabata, Y.; Ito, Y.; Tagawa, S. *CRC Handbook of Radiation Chemistry*; CRC Press: Boca Raton, FL, 1991.

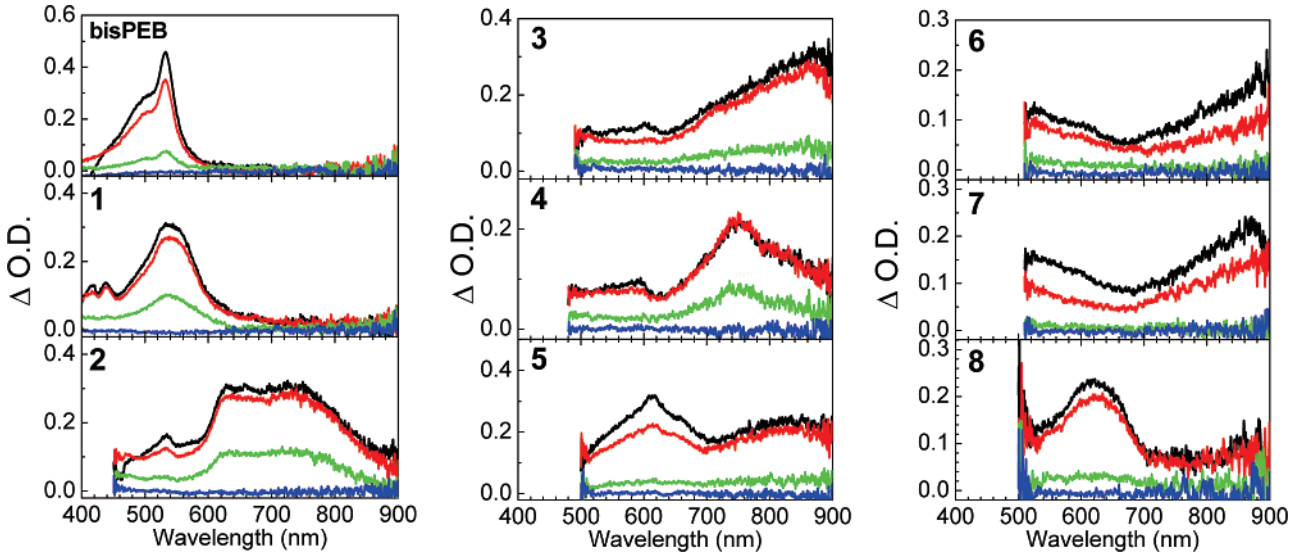

FIGURE 7. Time-resolved transient absorption spectra observed at time $t = 100$ ns (black), 1 (red), 10 (green), and 100 μs (blue) after an electron pulse during the pulse radiolysis of TPEBs (**1**−**8**) and bisPEB (0.5 mM) in Ar-saturated Bz.

were measured by cyclic voltammetry. We have reported that the annihilation enthalpy change ($-\Delta H°$) value for the charge recombination between $M^{\bullet+}$ and $M^{\bullet-}$ is criterion for whether $^1M^*$ can be formed by the charge recombination or not.[2,4] This $-\Delta H°$ value is calculated by eq 1[10]

$$-\Delta H° = [(E_{ox} - E_{red})]^{\epsilon}s - \Delta G_{sol}{}^{\epsilon}s - w_{a,\mu} + T\Delta S° \quad (1)$$

where E_{ox} and E_{red} are the oxidation and reduction potentials of M, respectively. ϵ_s, ΔG_{sol}, and $w_{a,\mu}$ represent the static dielectric constant of solvent, the free energy change of solvation, and the work required to bring $M^{\bullet+}$ and $M^{\bullet-}$ within a likely separation distance, respectively. For TPEBs and bisPEB in Bz, $-\Delta H°$ can be expressed using E_{ox} and E_{red} measured in CH_3CN by simplified eq 2

$$-\Delta H° = E_{ox} - E_{red} + 0.19 \text{ eV} \quad (2)$$

The calculated $-\Delta H°$ values for TPEBs and bisPEB are listed in Table 3, together with their oxidation and reduction potentials. The excitation energy of the S_1 state (E'_{S1}) was determined from the intersection point of the normalized spectra for absorption and radiolysis induced emission and listed in Table 3. $-\Delta H°$ values for all TPEBs and bisPEB (2.64−3.92 eV) are consistently larger than their E'_{S1} values (1.94−3.30 eV), indicating that the energy available in the charge recombination is sufficient to populate all TPEBs and bisPEB in the S_1 state.

As shown in Figure 6, the radiolysis induced emission intensity seems to be proportional to ϕ_{fl} value. However, the emission intensity of **5** (140) was higher than those of **3** (136) and **4** (104) although the ϕ_{fl} value of **5** (0.53) was lower than those of **3** (0.73) and **4** (0.62). It should be noted that the energy difference between $-\Delta H°$ and E'_{S1} ($-\Delta H° - E'_{S1}$) values for **5** (0.62 eV) was relatively higher than for **3** (0.36 eV) or **4** (0.45 eV) (Table 3). Consequently, it is proposed that the radiolysis induced emission intensity of TPEBs depends on both the ϕ_{fl} and ($-\Delta H° - E_{S1}$) values.

Transient Absorption Spectra Observed during Pulse Radiolysis of TPEBs. Figure 7 shows the transient absorption spectra observed during pulse radiolysis of TPEBs and bisPEB in Ar-saturated Bz (0.5 mM). For donor−acceptor-substituted TPEBs (**3**−**8**), the absorption bands at around 400−500 nm were not measured due to the strong ground-state absorption. The transient absorption was quenched during the pulse radiolysis of TPEBs in air-saturated Bz. In addition, these spectra were different from those observed in Ar-saturated 1,2-dichloroethane (DCE)[12,14] or *N*,*N*-dimethylformamide (DMF)[13,14] (Figures S1 and S2, Supporting Information), which can be assigned to $TPEB^{\bullet+}$ and $TPEB^{\bullet-}$, respectively. Therefore, the transient absorption spectra, observed during the pulse radiolysis of TPEBs in Ar-saturated Bz, are assigned to $^3TPEB^*$.[9] Since the time profile of each $^3TPEB^*$ decayed with second-order kinetics,[9] it is assumed that $^3TPEB^*$ mainly deactivates via triplet−triplet annihilation with no delayed fluorescence.

Little or no emission was observed during the pulse radiolysis of TPEBs in DCE and DMF, indicating that $TPEB^{\bullet+}$ and $TPEB^{\bullet-}$ do not emit light. In other words, both $TPEB^{\bullet+}$ and $TPEB^{\bullet-}$ must be formed at the same time in order to emit light. In Bz, however, no transient absorption band of $TPEB^{\bullet+}$ and $TPEB^{\bullet-}$ was observed immediately after an 8-ns electron pulse. Therefore, it is assumed that $TPEB^{\bullet+}$ and $TPEB^{\bullet-}$ immediately recombine to give $^1TPEB^*$ and $^3TPEB^*$, and $^1TPEB^*$ emits light within a pulse duration.[9] The passage of ionizing radiation through a liquid medium generates a series of isolated energy-deposition events, each of which develops a cluster of highly reactive species called a "spur". The radius of this spur is known

SCHEME 2. Proposed Mechanism of the Emission during the Pulse Radiolysis of TPEBs in Bz[a]

$$Bz \rightsquigarrow e^- + Bz^{\bullet+}$$

$$Bz^{\bullet+} + e^- \rightarrow Bz^*$$

$$Bz^{\bullet+} + TPEB \rightarrow TPEB^{\bullet+}$$

$$e^- + TPEB \rightarrow TPEB^{\bullet-}$$

$$TPEB^{\bullet+} + TPEB^{\bullet-} \rightarrow {}^1TPEB^* + TPEB \text{ and } {}^3TPEB^* + TPEB \text{ (within pulse duration (8 ns))}$$

$${}^1TPEB^* \rightarrow TPEB + h\nu_{fl} \ (\tau_{fl} < 8 \text{ ns})$$

$${}^3TPEB^* + {}^3TPEB^* \rightarrow 2TPEB \ (< 1 \ \mu s)$$

[a] For Donor−acceptor-substituted TPEBs (**3**−**8**), $^1TPEB^* = {}^1(A^{\bullet-}-D^{\bullet+})^*$ (ICT Character).

SCHEME 3. Proposed Structure for the Formation of TPEBs (1−8) in the S_1 and T_1 States during Pulse Radiolysis in Bz

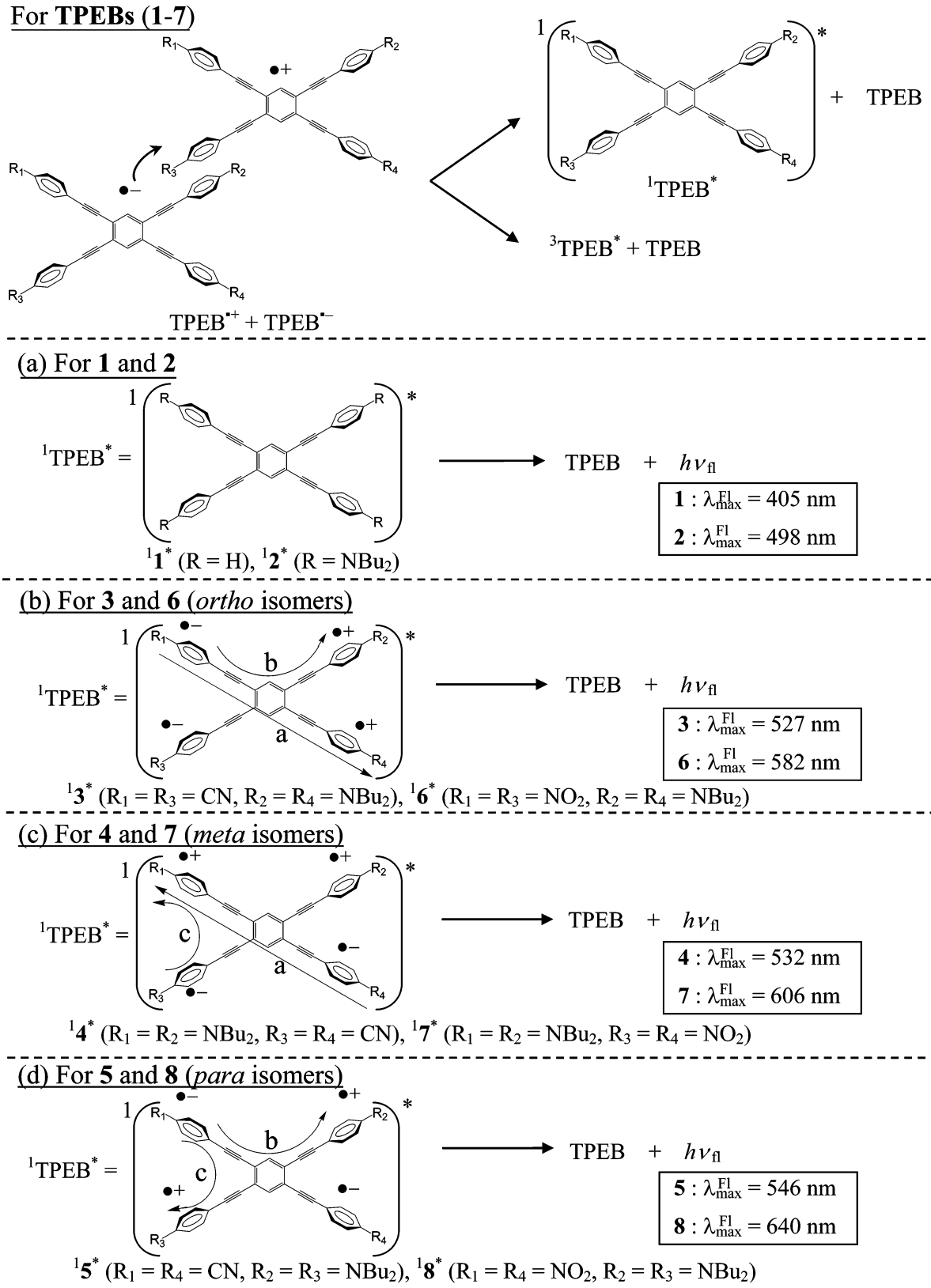

as 20−30 Å. Since the concentration of the reactive species within the spur is estimated to be high (of the order of 0.1 M), there is a relatively high probability for reacting with each other before they diffuse out into the bulk of the solution. Assuming that $TPEB^{\bullet+}$ and $TPEB^{\bullet-}$ undergo the charge recombination in the spur, the lifetime of the radical ions should be equivalent to the pulse duration. As far as we know, there are no reports on the charge recombination between radical ions within the

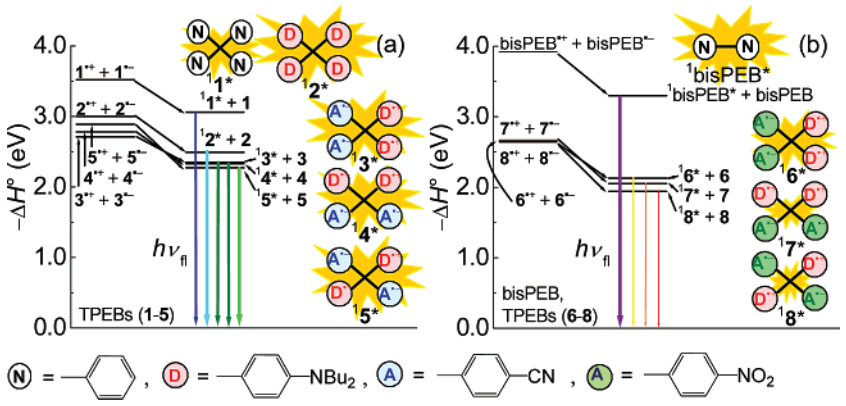

FIGURE 8. Energy level diagram for radiolysis induced chemiluminescence of TPEBs (**1**−**5** (a) and **6**−**8** (b)) and bisPEB (b). **N**, **D**, and **A** denote neutral-, electron donor-, and electron acceptor type molecules, respectively. $\mathbf{D}^{\bullet+}$ and $\mathbf{A}^{\bullet-}$ denote **D** radical cation and **A** radical anion, respectively.

spur. As the similar examples, however, the reactive species in the aqueous solution such as ($^{\bullet}OH$, e_{aq}^{-}, and $^{\bullet}H_3O$) are known to react with solutes such as (H^+, NO_3^-, N_2O, NO, O_2, H_2O_2, I^-, Tl^+, OH^-, $Fe(CN)_6^{4-}$, NO_2^-, etc.) within the spur.[14]

Emission Mechanism. A plausible mechanism of the emission during the pulse radiolysis of TPEBs in Bz is shown in Scheme 2. The same emission mechanism was assumed for bisPEB.

Thus, it is clarified that the charge recombination between $TPEB^{\bullet+}$ and $TPEB^{\bullet-}$ occurs to give $^1TPEB^*$ during the pulse radiolysis of TPEBs in Bz. The results obtained in this study indicate that the mechanism for the emission is quite different from those of DEAs.[9] TPEBs showed only monomer emission, while some DEAs showed both monomer and excimer emissions. For DEAs, it is suggested that enhancement of the π-conjugated system promotes the π-stacked excimer structure due to the ethynyl bond between donor and acceptor moieties. On the other hand, no excimer emission was observed for TPEBs. Because of the considerable repulsion between the substituents induced by the rotation around C−C single bonds, a π-stacked structure cannot be formed for the interaction between $TPEB^{\bullet+}$ and $TPEB^{\bullet-}$. Therefore, it is suggested that the geometries of radical cation and anion also affect the formation of the emissive species.

Although DEAs possess only a linear-conjugated pathway, donor−acceptor substituted TPEBs can contain three types of conjugated pathways: linear-conjugated (path a), cross-conjugated (path b), and "bent" conjugated (path c) pathways, as shown in Figure 1. The emission spectra of $^1TPEBs^*$ with ICT character depends on the substitution pattern and identities of the donor and acceptor groups during the pulse radiolysis. The radiolysis-induced emission spectra of all TPEBs showed the emission band in the region of wavelength where the fluorescence bands were observed by the steady-state measurements. Therefore, for neutral **1** and tetradonor **2**, it is suggested that $^1TPEB^*$ with π^*-antibonding character is formed by the charge recombination between $TPEB^{\bullet+}$ and $TPEB^{\bullet-}$, as shown in Scheme 3a. On the other hand, for ortho- (**3** and **6**), meta- (**4** and **7**), and para-substituted isomers (**5** and **8**), it is suggested that the charge recombination between $TPEB^{\bullet+}$ and $TPEB^{\bullet-}$ occurs to form $^1TPEB^*$ with ICT character as shown in parts b−d, respectively, of Scheme 3. Compared to ortho isomers, a slight red shift of the emission maxima was observed for the corresponding meta isomers (**3**: 527 nm vs **4**: 532 nm; **6**: 582 nm vs **7**: 606 nm), indicating the "bent" conjugated pathway (path c) leads the emission bands to the longer wavelength than cross-conjugated pathway (path b). In addition, it is also found that the emission intensities of meta isomers are lower than those of the corresponding ortho isomers (**3**: 136 vs **4**: 104; **6**: 52.1 vs **7**: 0.630). Compared to ortho and meta isomers, para isomers showed a further red shift (**3**: 527 and **4**: 532 nm vs **5**: 546 nm; **6**: 582 and **7**: 606 nm vs **8**: 640 nm). These results indicate cross-conjugated (path b) and "bent" conjugated (path c) pathways result in emission bands at longer wavelengths than in the linear-conjugated (path a).[15] Except for the emission efficiency of **5**, the photophysical properties observed during the pulse radiolysis of TPEBs were almost the same as those by the steady-state measurement.

Energy level diagrams for the radiolysis induced chemiluminescence of TPEBs and bisPEB are shown in Figure 8. It is evident that judicious choice of the donor/acceptor unit permits control of the HOMO−LUMO energy gap, and thus the emission wavelengths, can be tuned in the visible region (λ_{fl} = 360−800 nm). Different donor (NBu_2) and acceptor (CN and NO_2) substituents can change the emission color and intensity. Compared to TPEBs with electron-withdrawing CN substituents (**3**, **4**, and **5**), the emission maxima of TPEBs with stronger NO_2-acceptor substituents (**6**, **7**, and **8**) were observed at longer wavelengths. In addition, since the radiolysis induced emission intensity is assumed to be proportional to the ϕ_{fl} value, it is believed that the emission intensity of $^1TPEB^*$ with low-lying excitation energy (such as **7** and **8**) is reduced due to the increase of the internal conversion rate. Through control of the substituents of TPEBs, a broad range of emissions in the visible region can be achieved during pulse radiolysis.

Conclusions

Several substituted TPEBs show efficient monomer emission during pulse radiolysis in Bz. The emission is suggested to originate from $^1TPEB^*$, generated from charge recombination between $TPEB^{\bullet+}$ and $TPEB^{\bullet-}$, which are yielded from the initial radiolytic reaction. This mechanism is reasonably explained by the fact that the $-\Delta H°$ values (2.64−3.52 eV) estimated for the charge recombination between $TPEB^{\bullet+}$ and $TPEB^{\bullet-}$ are sufficiently larger than E'_{S1} of TPEBs (1.94−3.06 eV). The radiolysis induced emission spectra of TPEBs showed an obvious difference between each substitution pattern of the donor and/or acceptor groups. Since the HOMO−LUMO levels of TPEBs are changed with the substitution pattern and various

kinds of donor and acceptor groups (which induce the different types of charge-transfer pathways), fine-tuning of the emission color and intensity of donor−acceptor substituted TPEBs can be easily carried out. The efficient emission properties of this type of π-conjugated donor−acceptor molecule can be applicable as electroluminescent materials for OLEDs. Additional TPEB topologies are currently under investigation and their emissive properties will be reported in due course.

Experimental Section

Materials. 1,4-Bis(phenylethynyl)benzene (bisPEB) was purchased and purified by recrystallization from ethanol before use. TPEBs **1**, **2**, and **6**−**8** were prepared according to the procedure previously described in the literature.[6b] Although briefly described in an earlier communication,[6a] a new synthesis of TPEBs **3**−**5** is outlined in the Supporting Information and reflects the modular approach currently utilized for TPEB construction.

Measurements of Steady-State Spectral Properties. UV spectra were recorded in Bz with a UV/vis spectrometer using a transparent rectangular cell made from quartz (1.0 × 1.0 × 4.0 cm, path length of 1.0 cm). Fluorescence spectra were measured by a spectrofluorometer. The fluorescence quantum yields (ϕ_{fl}) were determined by using 9,10-diphenylanthracene[16a] (ϕ_{fl} = 0.90 in cyclohexane, λ_{ex}= 360 nm) and coumarin 334[16b] (ϕ_{fl} = 0.69 in methanol, λ_{ex}= 400 nm) standards.

Measurements of Electrochemical Properties. Oxidation (E_{ox}) and reduction potentials (E_{red}) were measured by cyclic voltammetry with platinum working and auxiliary electrodes and an Ag/Ag^+ reference electrode at a scan rate of 100 mV s^{-1}. Measurements were performed in dry CH_3CN containing approximately 1 mM of TPEBs and 0.1 M tetraethylammonium perchlorate. All TPEBs showed reversible oxidation and reversible reduction peaks.

Pulse Radiolysis. Pulse radiolysis experiments were performed using an electron pulse (28 MeV, 8 ns, 0.87 kGy per pulse) from a linear accelerator at Osaka University. All the sample solutions were prepared in a 0.5−10 mM concentration in Bz, 1,2-dichloroethane (DCE), or *N*,*N*-dimethylformamide (DMF) in a rectangular quartz cell (0.5 × 1.0 × 4.0 cm, path length of 1.0 cm). These solutions were saturated with Ar gas by bubbling for 10 min at room temperature before irradiation. The kinetic measurements were performed using a nanosecond photoreaction analyzer system. The monitor light was obtained from a pulsed 450-W Xe arc lamp, which was operated by a large current pulsed-power supply that was synchronized with the electron pulse. The monitor light was passed through an iris with a diameter of 0.2 cm and sent into the sample solution at a perpendicular intersection to the electron pulse. The monitoring light passing through the sample was focused on the entrance slit of a monochromator and detected with a photomultiplier tube. The transient absorption and emission spectra were measured using a photodiode array with a gated image intensifier as a detector. All emission spectra were corrected for the spectral sensitivity of the apparatus. To avoid pyrolysis of the sample solution by the monitor light, a suitable cutoff filter was used.

Fluorescence Lifetime Measurements. Fluorescence lifetimes were measured by the single photon counting method using a streakscope equipped with a polychromator. Ultrashort laser pulse was generated with a Ti:sapphire laser (fwhm 100 fs) pumped with a diode-pumped solid-state laser. For the excitation of samples, the output of the Ti:sapphire laser was converted to the second- (400 nm) or third harmonic oscillations (300 nm) with a harmonic generator.

Acknowledgment. We thank the members of the Radiation Laboratory of SANKEN, Osaka University, for running the linear accelerator. This work has been partly supported by a Grant-in-Aid for Scientific Research (Project 17105005, Priority Area (417), 21st Century COE Research, and others) from the Ministry of Education, Culture, Sports, Science and Technology (MEXT) of Japanese Government and the US National Science Foundation (CHE-0414175). E.L.S. acknowledges the NSF for an IGERT fellowship (DGE-0114419 and 0549503).

Supporting Information Available: Time-resolved transient absorption spectra observed during the pulse radiolysis of TPEBs in Ar-saturated DCE and DMF (5 mM); experimental procedures and copies of ^1H NMR spectra for **3**−**5**. This material is available free of charge via the Internet at http://pubs.acs.org.

JO062326H

(15) Moonen, N. N. P.; Diederich, F. *Org. Biomol. Chem*. **2004**, *2*, 2263.

(16) (a) Scaiano, J. C. *Handbook of Organic Photochemistry*; CRC Press: Boca Raton, FL, 1989; Vol. 1, p 231. (b) Reynolds, G. A.; Drexhage, K. H. *Optics Commun.* **1975**, *13*, 222.